Biomaterials Translational

Optimising soft tissue in-growth *in vivo* in additive layer manufactured osseointegrated transcutaneous implants

Elena Giusto[1,2,], Gordon Blunn[1,3], Roberta Ferro de Godoy[1,4], Chaozong Liu[1], Catherine Pendegrass[1]*

Key Words:
in-vivo model; ITAP; orthopaedic implants; osseointegrated transcutaneous implants

From the Contents

ABSTRACT

Osseointegrated transcutaneous implants could provide an alternative and improved means of attaching artificial limbs for amputees, however epithelial down growth, inflammation, and infections are common failure modalities associated with their use. To overcome these problems, a tight seal associated with the epidermal and dermal adhesion to the implant is crucial. This could be achieved with specific biomaterials (that mimic the surrounding tissue), or a tissue-specific design to enhance the proliferation and attachment of dermal fibroblasts and keratinocytes. The intraosseous transcutaneous amputation prosthesis is a new device with a pylon and a flange, which is specifically designed for optimising soft tissue attachment. Previously the flange has been fabricated using traditional machining techniques, however, the advent of additive layer manufacturing (ALM) has enabled 3-dimensional porous flanges with specific pore sizes to be used to optimise soft tissue integration and reduce failure of osseointegrated transcutaneous implants. The study aimed to investigate the effect of ALM-manufactured porous flanges on soft tissue ingrowth and attachment in an in vivo ovine model that replicates an osseointegrated percutaneous implant. At 12 and 24 weeks, epithelial downgrowth, dermal attachment and revascularisation into ALM-manufactured flanges with three different pore sizes were compared with machined controls where the pores were made using conventional drilling. The pore sizes of the ALM flanges were 700, 1000 and 1250 µm. We hypothesised that ALM porous flanges would reduce downgrowth, improve soft tissue integration and revascularisation compared with machined controls. The results supported our hypothesis with significantly greater soft tissue integration and revascularisation in ALM porous flanges compared with machined controls.

***Corresponding author:**
Elena Giusto,
elena.giusto@aol.com.

http://doi.org/10.12336/biomatertransl.2022.04.004

How to cite this article:
Giusto, E.; Blunn, G.; de Godoy, R.; Liu, C.; Pendegrass, C. Optimising soft tissue in-growth *in vivo* in additive layer manufactured osseointegrated transcutaneous implants. *Biomater Transl.* **2022**, *3*(4), 243-249.

Introduction

Amputation because of diabetes, neoplasia, traumatic injury, or infection is a common procedure. Stump-socket prostheses are used to restore missing limb function and improve patient quality of life and relative autonomy.[1] Many amputees find using conventional stump-socket devices challenging because the stump is unable to withstand weightbearing.[2, 3] Friction and perspiration at the skin-socket interface frequently cause pain, skin ulceration, breakdown, stump remodelling and infection.[4-6] As a result, a significant number of amputees abandon artificial limb use altogether.[7, 8]

Intraosseous transcutaneous amputation prostheses (ITAPs) were designed to overcome these problems and providing a secure attachment for artificial limbs. ITAP consists of an osseointegrated stem and a transcutaneous abutment that protrudes through the skin at the distal margin of the amputation stump, to which the artificial limb can be attached, transferring the mechanical ambulation forces directly to the bone in a more physiological manner.[9-13] ITAP has a flange incorporated in the region that traverses the epidermis and dermis of the skin. The flange was designed for soft tissue integration, to prevent downgrowth, subsequent infection and implant failure.[13-15] The concept of ITAP

evolved from looking at biomimetic models of transcutaneous devices. The three-dimensional (3D) porous structure of deer antlers, provides such a model,[16] with a transcutaneous porous interface (pedical bone) that facilitates soft tissue ingrowth and attachment through 'Sharpey's-like' collagen fibres, creating a tight infection-resistant seal.[16, 17] These characteristics were recapitulated as optimally as possible with manufacturing techniques available at the time. They resulted in an initial ITAP design, which incorporated a bi-dimensional machined flange (CM) with 700 μm drilled pores and a hydroxyapatite coating.[15] This solution was investigated in a previous clinical study (not yet published) and proved successful in a number of patients. However, in a few cases, the skin-implant interface was not completely infection-resistant resulting in superficial skin infection, and the relatively sharp edges of the drilled pores caused some inflammation of the skin.[18]

This study aimed to investigate a novel ITAP flange design that more closely mimics the 3D inter-connecting porous pedical bone seen to successfully support a transcutaneous interface in deer antler. The flange structure was generated using 3D-additive layer manufacturing (ALM) to create porous flanges with three different porosities (700, 1000 and 1250 μm). These porosities recapitulate the range of pore sizes observed within the pedical bone of deer antlers, creating an interconnecting porous structure. It was hypothesised that the ALM porous flanges would reduce epithelial downgrowth at a significant rate and improve dermal adhesion and revascularisation compared with CM controls.

Methods

Implant design and manufacture

Implants made of titanium alloy with porous 3D ALM flanges were obtained and printed by Eurocoatings (Trento, Italy) with pore dimensions of 700, 1000 and 1250 μm. Commercially machined flanged implants with 700 μm diameter drilled pores (as used in our previous clinical trial) served as controls (CM) (**Figure 1**). All implants were 60 mm total length and had a 5 mm abutment diameter. The 3D ALM printed porous flanges were 3 mm thick and 15 mm in diameter. The bone-anchored portion of the implants consisted of an M5 self-tapping screw thread. The CM control bone anchored part was coated with hydroxyapatite (Accentus Medical, Didcot Oxfordshire, UK) as previously used in our clinical study.[19] The stem's different designs were used taking into consideration the possibility of an influence in the soft tissue integration, however, the study was carried out at 12 and 24 weeks, a time point where variables such as the aseptic loosening are not yet visible.[20, 21] The 3D ALM porous flanges were not coated with hydroxyapatite as previously as it would have obscured the pores in the flange, preventing tissue ingrowth.

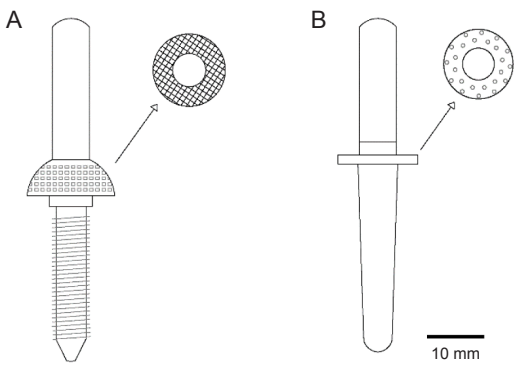

Figure 1. (A) An example of an ALM ITAP with a porous 3D flange. (B) An example of a CM Control ITAP with a drilled flanged.

Animal model and sample size calculation

All animal work was done under the Animals Scientific Act 1986, and in conjunction with the Royal Veterinary College's Animal Welfare and Ethical Review Body. Ten adult female ewes (breed; mules) were sedated pre-operatively (intramuscular, xylazine hydrochloride 0.2 mg/kg; Bayer Plc., Suffolk, UK). Anaesthesia was induced with intravenous midazolam (2.5 mg stat dose; Roche Products Ltd., Welwyn Garden City, UK) and ketamine hydrochloride, and maintained with 3% halothane (Merial Animal Health Ltd., Harlow, UK) and oxygen (4 L/min). The medial aspect of the right tibia was isolated in a sterile field and for each implant, a 7 mm skin incision was made. A periosteal elevator was used to expose the underlying bone and a 4 mm hole was drilled through both cortices of the tibia prior to inserting the self-tapping device. The implant was inserted using a hand-held T-bar. One of each 700, 1000 and 1250 μm pore ALM and CM control implants were surgically implanted transversally into the tibia as shown in **Figure 2** where positions 1–4 corresponded to the sites of implants. The implants were positioned at intervals of 3–4 cm, and their position relative to the proximal end of the tibia was rotated to ensure that, in every four animals, the implant design was in a different position. This was performed to account for differences in the soft tissue thickness variation over the length of the tibia. The flanges were positioned on the surface of the bone below the skin. The wound was closed

1 Institute of Orthopaedic & Musculoskeletal Science, University College London, Royal National Orthopaedic Hospital, Stanmore, UK; 2 Barts and the London School of Medicine and Dentistry, Queen Mary University London, London, UK; 3 School of Pharmacy and Biomedical Sciences, University of Portsmouth, Portsmouth, UK; 4 Writtle University College, Writtle, UK

in two layers using interrupted Vicryl 2-0 resorbable sutures. The first layer of subdermal fascia, was closed over the flange, followed by skin sutures to seal the soft tissue around the transcutaneous abutment. The animals freely moved straight after the surgery, dressings were changed daily for 7 days and wound sites were checked weekly for signs of inflammation, infection and implant loosening. All animals were housed in individual pens for the first post-operative week and then moved to group housing (n = 4 per group) thereafter for the duration of the study. Animals were euthanised at 12 (n = 5) and 24 weeks (n = 5).

Sample size was calculated using Mead's resource equation[22] rearranged to give n (number of subjects per group) = DF/k + 1 (DF = degrees of freedom (considered to be 10 and 20 to give a minimum and maximum n number respectively), k = number of groups). This yielded a minimum and maximum n of 4 (rounded up from 3.5) and 6 subjects per group, respectively. Hence n of 5 was considered appropriate to provide data able to demonstrate significant differences should they exist.

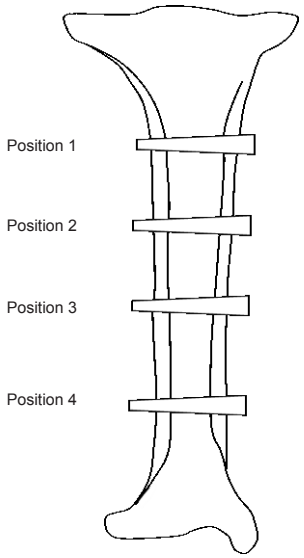

Figure 2. Position of implants on sheep tibia.

Histological processing and image analysis

The animals underwent euthanasia using intravenous 0.7 mg/kg pentobarbital solution (Pharmasol Ltd., Andover, UK). The medial aspect of the tibia was exposed and a square of soft tissue, a minimum of 1 cm from the edge of the flange, was incised down to the underlying bone. A hand-held saw was used to remove. The implant with the surrounding square of soft tissue and the underlying tibial bone, were removed using a hand-held saw. While the implants where retrieved, a great attention was used to avoid any disruption on skin. The specimens were left in 10% formal saline for 7 days, and eventually embedded in LR White resin (London Resin Company Limited, Reading, UK) after 5 days alcohol dehydratation. Sections were cut through the centre of the implants (Exakt E310 diamond band saw (Mederex, Frame, UK)), ground, and polished to 100 μm (Exakt-Micro-Grinding System, Mederex), stained with toluidine blue and paragon, and analysed using a Carl Zeiss microscope linked to Axiovision Rel 4.5 Image Analysis software (Carl Zeiss, Oberkochen, Germany). Quantitative analysis was performed using measures of downgrowth, % epithelial layer attachment and % soft-tissue (sub-epithelial dermal) layer attachment. Epithelial downgrowth was measured by drawing and measuring a line from the skin surface to the position where the epithelium was observed to end, at the epithelial layer – implant interface The percentage of epithelial and sub-epithelial attachment to the pylon was determined using a line method to measure the thickness of the epithelial and sub-epithelial tissue layers, and the percentage of those layers in contact with the implant surface was calculated. For the sub-epithelial tissue and blood vessel distribution, this process was performed at one third intervals across the width of the flange, and an average calculated. The number of blood vessels were counted in 1 mm^2 regions at each of the one third width intervals within the tissue. An average value was used for data analysis.

Statistical analysis

The data were analysed in SPSS (version 24.0 for windows, IBM, Armonk, NY, USA). For each analysis, data for CM controls were compared with each of the 700, 1000 and 1250 μm pore ALM implants. In addition, comparisons between the ALM implant data were also performed. The data did not fit the assumption required for parametric testing, hence non-parametric analyses were used. Results are presented as median values (with 95% confidence intervals). For multiple comparative analyses of implant types, the Kruskal-Wallis H test was performed. Where a difference was observed, pair-wise Mann-Whitney U tests were used to determine differences between individual implant types. Analyses were carried out between implant types at 12 and 24 weeks, and within each implant type between 12 and 24 weeks. Significance was assumed at the 0.05 level.

Results

Epithelial downgrowth

Epithelial downgrowth – 12 weeks

After 12 weeks, the downgrowth for the 700 μm, 1000 μm, 1250 μm and CM implants were 2385.69 μm (585 – 4264.02 μm), 1040.51 μm (1137 – 2259.9 μm), 2682.6 μm (947 – 2129.15 μm) and 1756.19 μm (514 – 1756.6 μm) respectively.

No significant differences were observed in epithelial downgrowth for all the implant types ($P = 0.289$). However, the implant type with the lowest degree of epithelial downgrowth was the ALM 1000 μm porous flange.

Epithelial downgrowth – 24 weeks

After 24 weeks, the downgrowth for the 700 μm, 1000 μm, 1250 μm and CM implants were 2342.2 μm (2288.5 – 3070 μm), 2609.5 μm (1848 – 3698 μm), 3037.6 μm (2093 – 4212 μm) and 1159.1 μm (1263.4 – 1679.7 μm) respectively.

By 24 weeks, the Kruskal-Wallis *H* test demonstrated that the data were not from the same population distribution ($P = 0.021$). Pair-wise Mann-Whitney *U* test showed significantly greater epithelial downgrowth around the ALM implants with 700 μm and 1250 μm porous flanges compared with CM controls ($P = 0.015$ and $P = 0.015$, respectively).

Epithelial downgrowth between 12 and 24 weeks

No significant differences were observed between 12 and 24 weeks for any of the implant types tested (all $P > 0.05$).

Percentage of epithelial attachment on pylon

Epithelial attachment – 12 weeks

After 12 weeks, the epithelial attachment to the 700, 1000, 1250 μm and CM implants were 51.9% (0 – 90%), 43% (0 – 78%), 60.5% (17 – 95.5%) and 24.5% (10 – 36.5%) respectively.

At 12 weeks, the Kruskal-Wallis *H* test indicated that the ALM and CM implant data were not from the same population distribution ($P = 0.014$). Paired-wise Mann-Whitney *U* tests showed significantly higher levels of epithelial attachment to the 700 ($P = 0.019$), 1000 ($P = 0.019$) and 1250 μm ($P = 0.025$) porous implants respectively compared with the controls. This demonstrates that epithelial attachment is significantly greater around all ALM implants compared with CM controls.

Epithelial attachment – 24 weeks

After 24 weeks, the epithelial attachment percentages on 700, 1000, 1250 μm and CM implants, were 53.5% (17.5 – 97%), 29% (15 – 54%), 59.2% (17 – 90%), and 34.2% (0 – 61%) respectively.

Pair-wise Mann-Whitney *U* tests demonstrated significantly higher values were obtained between 700 and 1000 μm porous implants ($P = 0.030$) and for the 700 μm porous implant and CM controls ($P = 0.024$).

The data analyses demonstrate that epithelial attachment around the 700 μm pore ALM implants was significantly greater compared with CM controls.

Epithelial attachment between 12 and 24 weeks

Data for each implant type were compared between 12 and 24 weeks, however, no significant differences were observed ($P > 0.05$).

Percentage of sub-epithelial attachment after 12 and 24 weeks

Sub-epithelial attachment – 12 weeks

After 12 weeks, the median percentage of sub-epithelial attachment was significantly higher for porous implants compared with CM controls, irrespective of pore size (all $P < 0.05$). The attachment for 700, 1000, 1250 μm and CM were 90.7% (72.9 – 100%), 90.8% (82 – 100%), 71.3% (91 – 100%) and 81.6% (71.5 – 100%), respectively.

A Kruskal-Wallis *H* test demonstrated a significant difference in the data sets ($P = 0.007$). Pair-wise Mann-Whitney *U* tests showed significantly higher sub-epithelial attachment around porous implants with 1000 μm pores compared with 1250 μm ($P = 0.004$). Sub-epithelial attachment to all porous implants was significantly greater compared with the CM control, irrespective of pore size ($P = 0.001$). After 12 weeks, a significant greater sub-epithelial attachment was observed around porous implants with 1000 μm ($P = 0.004$) and 1250 μm ($P = 0.003$) pores, compared with the CM controls.

Sub-epithelial attachment – 24 weeks

After 24 weeks, the percentage of sub-epithelial attachment for 700, 1000, 1250 μm and CM implants was 97.2% (86 – 100%), 88.9% (69 – 100%), 79% (58 – 100%) and 77.6% (0 – 100%) respectively.

The 24 weeks median comparison within implants, showed a greater level of sub-epithelial adhesion for 1000 ($P = 0.004$) and 1250 μm ($P = 0.004$) compared with CM controls.

Sub-epithelial attachment after 12 and 24 weeks

Within implant analysis between 12 and 24 weeks showed non-significant differences.

Histological appearance

Figure 3 shows the histological appearance of the sub-epithelial tissues around 1250 μm porous flanges and CM control implants at 12 and 24 weeks. In both the 3D ALM porous implants, the dermis is well established within the metal meshes of the flange. All the flange meshes are in intimate contact with the sub-epithelial tissues. Blood vessels are also present within the new tissue formed and there is no indication of inflammation.

In contrast, the sub-epithelial tissues around CM control implants showed a large area of detachment on two sides of the drilled pore after 12 weeks, whilst gapping was observed on the top and side of the flange after 24 weeks. The connective tissue has a dense and homogeneous morphology, and no blood vessels were observed within the drilled pores of the CM control flanges.

Blood vessels distribution after 12 and 24 weeks

Blood vessel distribution – 12 weeks

The average number of blood vessels from one-third width

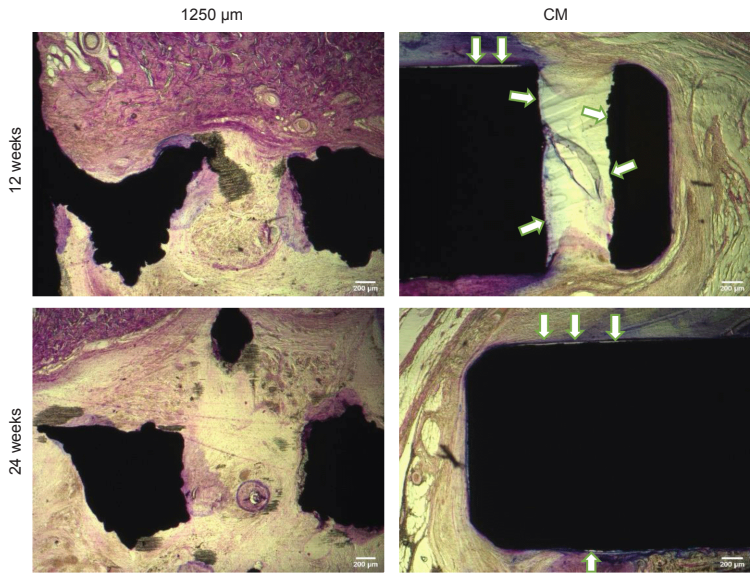

Figure 3. Representative images of histological sections picturing the dermal attachment to the flange at 12 and 24 weeks. The black part represents the metal flange in a transversal section surrounded by soft tissue. The arrows show the gap between the sub-epithelial tissue and the CM implant. Scale bars: 200 µm.

intervals across the whole implant were 23.3/mm^2 (10–31/mm^2), 19.2/mm^2 (8–30/mm^2), 22.3/mm^2 (10–30/mm^2) and 11.4/mm^2 (0–30/mm^2) for 700, 100, 1250 µm and CM controls, respectively.

The Kruskal-Wallis *H* test did not show any significant differences between the data ($P > 0.05$).

Blood vessel distribution – 24 weeks

The average number of blood vessels from one-third width intervals across the whole of each implant were 19.6/mm^2 (15–20/mm^2), 21.4/mm^2 (15–23/mm^2), 20.9/mm^2 (17–30/mm^2) and 6.2/mm^2 (0–30/mm^2) for 700, 100, 1250 µm and CM controls, respectively.

Pair-wise Mann-Whitney *U* tests showed a significantly greater number of blood vessels in the 700 µm pore flanges compared with CM controls ($P = 0.009$) and between 1000 µm flanges and CM controls ($P = 0.009$).

Blood vessel distribution between 12 and 24 weeks

Analysis of the number of blood vessels within each implant type between 12 and 24 weeks demonstrated that the number of blood vessels significantly decreased in CM controls between the two timepoints ($P = 0.03$). No other significant differences were observed.

Discussion

This study investigated the nature of the skin-implant interface between 3D ALM porous flanges and CM controls. Clinically, epithelial attachment and sub-epithelial tissue ingrowth to an osseointegrated transcutaneous implant (OTI) within the first two weeks are critical for preventing infection and maintaining a healthy and sealed tissue-implant interface.[23-27]

In this study, epithelial downgrowth was not significantly different between implant types at 12 weeks post-implantation. It was observed to be significantly greater (except for 1000 µm ALM implants) around porous implants by 24 weeks compared with CM controls. This may be considered detrimental to the transcutaneous interface, however, considering our positive findings for the analyses of sub-epithelial layer attachment and revascularisation around ALM implants, we postulate that this is not the case.

We detected pore-size-specific significant increases in percentage epithelial attachment, percentage sub-epithelial attachment, and revascularisation (as evidenced by the number of blood vessels per 1 mm^2) at both 12 and 24 weeks in porous ALM implants compared with CM controls.

Given these findings, we postulated that epithelial attachment might have been influenced by the position of the implants within the tibia, and the amount of overlying tissue and relative interfacial movements. Although the implant position was rotated within the tibia, the degree of epithelial downgrowth observed might have been exacerbated by the additional height of the porous flange within the soft tissues. In addition, the transverse implant position (adopted in our animal model), differs from the physiological one found in a clinically implanted OTI. The amount of tissue overlying an implant, and the degree to which the height of the flange influences the success of the transcutaneous interface need further investigation that may provide information for a clinical setting without the use of an animal amputation model.

The percentage of epithelial attachment was significantly higher around 3D ALM porous flanges after 12 and 24 weeks in comparison with CM Controls. This demonstrates, that despite increased epithelial downgrowth, the 3D ALM porous structure of the flange is beneficial. We postulate that the significantly greater degree of sub-epithelial layer attachment observed around porous implants compared with CM controls, is sufficient to prevent any further downgrowth (evidenced by the lack of any significant difference in epithelial downgrowth between 12 and 24 weeks around 3D ALM porous flanges) and

enhance epithelial layer attachment. In addition, the porous implant provides a greater space optimising dermal attachment compared with CM controls. One key aspect of the clinical success of OTIs, is the early adhesion of the epithelial layer to maintain an aseptic environment with limited movement at the interface. This dictates that in "the race for surface", where bacteria compete with the soft tissue to attach to the implant, the epithelial attachment is promoted ahead of bacterial colonisation.

Sub-cutaneous attachment to the 3D ALM porous flanges was significantly greater compared with CM controls and this was supported by the histological findings. The metal pores of the 3D ALM flanges were filled with soft tissue after 12 and 24 weeks, with revascularisation of the tissues within the pores of the 1000 and 1250 μm implants being significantly greater by 24 weeks. This finding further supports our hypothesis, demonstrating that the three-dimensional structure of the porous implants enhances cell attachment and tissue ingrowth. In fact, no encapsulation has been observed as previously described around OTIs.[13] We postulate that the 3D ALM flanges achieve this by providing a wider contact surface for cell and tissue adhesion compared with the CM controls.[28] Moreover, the forces at the tissue-implant interfaces throughout the 3D ALM porous structures are reduced because they are distributed over a wider surface area compared with those encountered in the CM controls. This diminishes the detrimental effect these forces have on the integrity of the transcutaneous seal.[29-31] Our findings also show that 3D ALM porous implants support improved revascularisation, which is critical for tissue regeneration,[25] which further consolidates our hypothesis.

We acknowledge that the transverse positioning of the implants within the tibiae was a limitation of this study, and that bacterial infection was not investigated here. However, at 24 weeks, the 3D ALM porous implants were supporting the transcutaneous interfaces with no evidence of progressing downgrowth. The interfaces had significantly greater levels of epithelial and sub-epithelial layer attachment and improved revascularization compared with CM controls. We also acknowledge that hydroxyapatite coating improved the previously published outcome comparing hydroxyapatite- and non-hydroxyapatite-coated plain flanges.[18] However, in this specific case, the pore size of the flanges, would have obscured the interconnecting porous structures defeating our point of investigation. Undoubtedly hydroxyapatite improves further the integration of the soft tissue within the flange if coated, but any improvement in soft tissue integration has the possibility of eliminating soft tissue-implant downgrowth and infection resulting in a positive outcome.

In summary, despite the drawbacks discussed here, our findings of increased epithelial and sub-epithelial attachment, and improved revascularisation around 3D ALM porous implants support their use in OTI technology.

Author contributions

Conceptualization: CP, GB; investigation: EG, RFG, GB, CP; data analysisand original manuscript draft: EG; manuscript review and editing: CP, CL, GB; funding acquisition: CP, GB, CL. All authors have read and agreed to the final version of the manuscript.

Financial support

This study was financially supported by a UCL Impact Studentship in collaboration with Fitzpatrick Referrals Ltd. (award No. 174064); European Commission via H2020 MSCA RISE BAMOS programme (project No. 734156); Versus Arthritis (project No. 21160); the Rosetree Trust (project No. A1184); and the Innovate UK via Newton Fund (No. 102872).

Acknowledgement

We would like to thank UCL Orthopaedic Bioengienering Research Group and Professor Hongwei Ouyang and his team at Zhejiang University for their support for this study.

Conflicts of interest statement

The authors declare no conflict of interests.

Editor note: Chaozong Liu is an Editorial Board member of B*iomaterials Translational*. He was blinded from reviewing or making decisions on the manuscript. The article was subject to the journal's standard procedures, with peer review handled independently of this Editorial Board member and his research group.

1. Adamson, C.; Kaufmann, M.; Levine, D.; Millis, D. L.; Marcellin-Little, D. J. Assistive devices, orthotics, and prosthetics. *Vet Clin North Am Small Anim Pract.* **2005**, *35*, 1441-1451, ix.
2. Ontario Health (Quality). Osseointegrated prosthetic implants for people with lower-limb amputation: a health technology assessment. *Ont Health Technol Assess Ser.* **2019**, *19*, 1-126.
3. Roffman, C. E.; Buchanan, J.; Allison, G. T. Predictors of non-use of prostheses by people with lower limb amputation after discharge from rehabilitation: development and validation of clinical prediction rules. *J Physiother.* **2014**, *60*, 224-231.
4. Pirouzi, G.; Abu Osman, N. A.; Eshraghi, A.; Ali, S.; Gholizadeh, H.; Wan Abas, W. A. Review of the socket design and interface pressure measurement for transtibial prosthesis. *ScientificWorldJournal.* **2014**, *2014*, 849073.
5. Bhandari, P. S.; Jain, S. K. Long term effects of prostheses on stump in lower limb amputees: a critical analysis of 100 cases. *Med J Armed Forces India.* **1996**, *52*, 169-171.
6. Bowker, J. H.; Michael, J. W. Atlas of limb prosthetics: surgical, prosthetic, and rehabilitation principles. Mosby Inc.: St. Louis, 1992.
7. National Health Service. Amputation. https://www.nhs.uk/conditions/amputation/. Accessed August 9, 2022.
8. Cole, G. L.; Millis, D. The effect of limb amputation on standing weight distribution in the remaining three limbs in dogs. *Vet Comp Orthop Traumatol.* **2017**, *30*, 59-61.
9. Tzortzis, S.; Tzifa, K.; Tikka, T.; Worrollo, S.; Williams, J.; Reid, A. P.; Proops, D. A ten-year review of soft tissue reactions around percutaneous titanium implants for auricular prosthesis. *Laryngoscope.* **2015**, *125*, 1934-1939.
10. Li, Y.; Felländer-Tsai, L. The bone anchored prostheses for amputees - historical development, current status, and future aspects. *Biomaterials.* **2021**, *273*, 120836.
11. Overmann, A. L.; Forsberg, J. A. The state of the art of osseointegration for limb prosthesis. *Biomed Eng Lett.* **2020**, *10*, 5-16.
12. Pitkin, M.; Cassidy, C.; Shevtsov, M. A.; Jarrell, J. R.; Park, H.; Farrell, B. J.; Dalton, J. F.; Childers, W. L.; Kistenberg, R. S.; Oh, K.; Klishko, A. N.; Prilutsky, B. I. Recent progress in animal studies of the skin- and

bone-integrated pylon with deep porosity for bone-anchored limb prosthetics with and without neural interface. *Mil Med.* **2021**, *186*, 688-695.
13. Isackson, D.; McGill, L. D.; Bachus, K. N. Percutaneous implants with porous titanium dermal barriers: an in vivo evaluation of infection risk. *Med Eng Phys.* **2011**, *33*, 418-426.
14. Tsikandylakis, G.; Berlin, Ö.; Brånemark, R. Implant survival, adverse events, and bone remodeling of osseointegrated percutaneous implants for transhumeral amputees. *Clin Orthop Relat Res.* **2014**, *472*, 2947-2956.
15. Fitzpatrick, N.; Smith, T. J.; Pendegrass, C. J.; Yeadon, R.; Ring, M.; Goodship, A. E.; Blunn, G. W. Intraosseous transcutaneous amputation prosthesis (ITAP) for limb salvage in 4 dogs. *Vet Surg.* **2011**, *40*, 909-925.
16. Kierdorf, U.; Flohr, S.; Gomez, S.; Landete-Castillejos, T.; Kierdorf, H. The structure of pedicle and hard antler bone in the European roe deer (Capreolus capreolus): a light microscope and backscattered electron imaging study. *J Anat.* **2013**, *223*, 364-384.
17. Pendegrass, C. J.; Goodship, A. E.; Blunn, G. W. Development of a soft tissue seal around bone-anchored transcutaneous amputation prostheses. *Biomaterials.* **2006**, *27*, 4183-4191.
18. Chimutengwende-Gordon, M.; Pendegrass, C.; Blunn, G. The in vivo effect of a porous titanium alloy flange with hydroxyapatite, silver and fibronectin coatings on soft-tissue integration of intraosseous transcutaneous amputation prostheses. *Bone Joint J.* **2017**, *99-b*, 393-400.
19. Kang, N. V.; Pendegrass, C.; Marks, L.; Blunn, G. Osseocutaneous integration of an intraosseous transcutaneous amputation prosthesis implant used for reconstruction of a transhumeral amputee: case report. *J Hand Surg Am.* **2010**, *35*, 1130-1134.
20. Anil, U.; Singh, V.; Schwarzkopf, R. Diagnosis and detection of subtle aseptic loosening in total hip arthroplasty. *J Arthroplasty.* **2022**, *37*, 1494-1500.
21. Abu-Amer, Y.; Darwech, I.; Clohisy, J. C. Aseptic loosening of total joint replacements: mechanisms underlying osteolysis and potential therapies. *Arthritis Res Ther.* **2007**, *9 Suppl 1*, S6.
22. Mead, R.; Gilmour, S. G.; Mead, A. Statistical principles for the design of experiments: applications to real experiments. Cambridge University Press: Cambridge. 2012.
23. Steinstraesser, L.; Sorkin, M.; Niederbichler, A. D.; Becerikli, M.; Stupka, J.; Daigeler, A.; Kesting, M. R.; Stricker, I.; Jacobsen, F.; Schulte, M. A novel human skin chamber model to study wound infection ex vivo. *Arch Dermatol Res.* **2010**, *302*, 357-365.
24. Pendegrass, C. J.; Gordon, D.; Middleton, C. A.; Sun, S. N.; Blunn, G. W. Sealing the skin barrier around transcutaneous implants: in vitro study of keratinocyte proliferation and adhesion in response to surface modifications of titanium alloy. *J Bone Joint Surg Br.* **2008**, *90*, 114-121.
25. Caiado, F.; Carvalho, T.; Silva, F.; Castro, C.; Clode, N.; Dye, J. F.; Dias, S. The role of fibrin E on the modulation of endothelial progenitors adhesion, differentiation and angiogenic growth factor production and the promotion of wound healing. *Biomaterials.* **2011**, *32*, 7096-7105.
26. Coulter, F. B.; Levey, R. E.; Robinson, S. T.; Dolan, E. B.; Deotti, S.; Monaghan, M.; Dockery, P.; Coulter, B. S.; Burke, L. P.; Lowery, A. J.; Beatty, R.; Paetzold, R.; Prendergast, J. J.; Bellavia, G.; Straino, S.; Cianfarani, F.; Salamone, M.; Bruno, C. M.; Moerman, K. M.; Ghersi, G.; Duffy, G. P.; O'Cearbhaill, E. D. Additive manufacturing of multi-scale porous soft tissue implants that encourage vascularization and tissue ingrowth. *Adv Healthc Mater.* **2021**, *10*, e2100229.
27. Overmann, A. L.; Aparicio, C.; Richards, J. T.; Mutreja, I.; Fischer, N. G.; Wade, S. M.; Potter, B. K.; Davis, T. A.; Bechtold, J. E.; Forsberg, J. A.; Dey, D. Orthopaedic osseointegration: Implantology and future directions. *J Orthop Res.* **2020**, *38*, 1445-1454.
28. Taniguchi, N.; Fujibayashi, S.; Takemoto, M.; Sasaki, K.; Otsuki, B.; Nakamura, T.; Matsushita, T.; Kokubo, T.; Matsuda, S. Effect of pore size on bone ingrowth into porous titanium implants fabricated by additive manufacturing: an in vivo experiment. *Mater Sci Eng C Mater Biol Appl.* **2016**, *59*, 690-701.
29. Chimutengwende-Gordon, N. F. Enhancing the soft tissue-implant seal and reducing bacterial colonisation around the intraosseous transcutaneous amputation prosthesis. University College London: College. 2015.
30. Akhmanova, M.; Osidak, E.; Domogatsky, S.; Rodin, S.; Domogatskaya, a. physical, spatial, and molecular aspects of extracellular matrix of in vivo niches and artificial scaffolds relevant to stem cells research. *Stem Cells Int.* **2015**, *2015*, 167025.
31. Ghilan, A.; Chiriac, A. P.; Nita, L. E.; Rusu, A. G.; Neamtu, I.; Chiriac, V. M. Trends in 3D printing processes for biomedical field: opportunities and challenges. *J Polym Environ.* **2020**, *28*, 1345-1367.

Received: August 24, 2022
Revised: September 28, 2022
Accepted: November 11, 2022
Available online: December 28, 2022